PROCEEDINGS, Thirty-Sixth Workshop on Geothermal Reservoir Engineering
Stanford University, Stanford, California, January 31 - February 2, 2011
SGP-TR-191

NUMERICAL MODELING OF ARTIFICIAL HYDRO-FRACTURES IN HOT DRY ROCK RESERVOIRS BY USING DISPLACEMENT DISCONTINUTY METHOD

Mahmoud Behnia [a], Kamran Goshtasbi [b] , Aliakbar Golshani [c], Mohammad Fatehi Marji [d]

[a,b] Department of mining Engineering, Faculty of Eng.,Tarbiat Modares University
[c] Department of Civil Engineering, Faculty of Eng., Tarbiat Modares University
[a,b,c] Jalal Ave., Tehran, Iran
[d] Faculty of Mining Engineering, Yazd University
Safaiyeh, Yazd, Iran
e-mail: mahmoud.behnia@modares.ac.ir

ABSTRACT

Artificial cracks are required for heat exchanging surface and/or flow paths in the hot dry rock reservoirs. Fracture mechanics is the only methodology that has been found effective in evaluating the size of artificial cracks, the surface area of the heat exchanger. In this study, fracture mechanics with boundary element method based on the displacement discontinuity formulation is presented to solve general problems of interaction between artificial hydro-fractures and discontinuities that are in the reservoir. The numerical results are in good agreement with the results brought in the literature. The comparison of numerical method with exact solution shows a good performance of the method in the case of interacting cracks too.

INTRODUCTION

Hydraulic fracturing has been used in the petroleum industry as a stimulation technique to enhance oil and gas recovery in low permeability reservoirs and for estimating in situ stresses (Clark, 1949). Its applications also include pressure grouting and disposal of granular or liquid waste underground and hot dry rock stimulation, (Albright and Pearson, 1982).

Hydraulic fracturing is a complex operation in which the fluid is pumped at high pressure into a selected section of the wellbore. The high-pressure fluid exceeds the tensile strength of the rock and initiates a fracture in the rock. The fracture will grow in the direction of least resistance and some distance away from the borehole the fracture will always propagate in the direction normal to the smallest principal stress in that specific formation(Ching,1997).

One of the important features needed in fracture design is the ability to predict the geometry and the characteristics of hydraulically induced fracture.

Because of the presence of discontinuities in the rock mass, a better understanding of how an induced fracture interacts with a discontinuity is fundamental for predicting the ultimate size and shape of the hydraulic fractures formed by a treatment. Theoretical and experimental investigations of fracture initiation, propagation, and interaction with pre-existing geological discontinuities based on fracture mechanics theory began during the 1960s and work continues on this topic.

In the fracture analysis of brittle substances (like most of the rocks), the Mode I and Mode II stress intensity factors can be calculated by numerical methods using ordinary element.

Boundary element method is one of the powerful numerical methods and has been extensively used in fracture mechanics (Aliabadi and Rooke, 1991; Aliabadi, 1998). Displacement discontinuity method (DDM) is an indirect boundary element method, which has been used for the analysis of crack problems related to rock fracture mechanics. It should be noted that DDM does not have the re-meshing problem.

The problem of crack tip singularities has been improved by the uses of one crack tip element for each crack tip and recently higher order elements have been used to increase the accuracy of the numerical results (Crawford and Curran, 1982; Shou and Crouch, 1995). Therefore, the higher order variation of the displacement discontinuities together with special crack tip elements are usually used for the treatment of crack problems (Scavia 1995; Shou and Crouch, 1995; Tan et. al. (1996); Marji et al., 2006; Hosseini-nasab and Marji, 2007 ; Marji M. F., Dehghani I., 2009).

In the present work, a general higher order displacement discontinuity method implementing crack tip element for each crack end is used to study of the interaction and coalescence of pressurized fractures. This paper shows how the crack tip interaction affects the behavior and geometry of the fractures, stress intensity factors (SIF) and crack opening displacement (COD) profile.
Some example problems are solved and the computed results are compared with the results given in the literature. The numerical results obtained here are in good agreement with those cited in the literature. The comparison of numerical method with exact solution shows a good performance of the method in the case of interacting cracks too.

HIGHER ORDER DISPLACEMENT DISCONTINUITY METHOD

A displacement discontinuity element with length of 2a along the x-axis is shown in Figure 1 (a), which is characterized by a general displacement discontinuity distribution of u(ε). By taking the u_x and u_y components of the general displacement discontinuity u(ε) to be constant and equal to D_x and D_y respectively, in the interval (-a, +a) as shown in Figure 1 (b), two displacement discontinuity element surfaces can be distinguished, one on the positive side of y ($y=0_+$) and another one on the negative side ($y=0_-$). The displacements undergo a constant change in value when passing from one side of the displacement discontinuity element to the other side. Therefore, the constant element displacement discontinuities D_x and D_y can be written as:

$$D_x = u_x(x,0_-) - u_x(x,0_+), D_y = u_y(x,0_-) - u_y(x,0_+) \qquad (1)$$

The positive sign convention of D_x and D_y is shown in Figure 1 (b) and demonstrates that when the two surfaces of the displacement discontinuity overlap D_y is positive, which leads to a physically impossible situation. This conceptual difficulty is overcome by considering that the element has a finite thickness, in its undeformed state, which is small compared to its length, but bigger than D_y (Crouch 1976; Crouch and Starfield 1983).

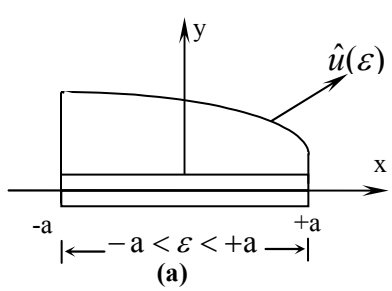

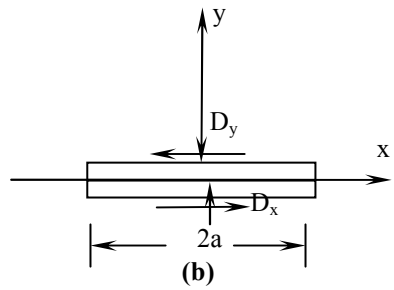

Fig. 1. a) Displacement discontinuity element and the distribution of u(ε). b) Constant element displacement discontinuity

Quadratic Element Formulation

The quadratic element displacement discontinuity is based on analytical integration of quadratic collocation shape functions over collinear, straight-line displacement discontinuity elements (Shou and Crouch 1995). Figure 2 shows the quadratic displacement discontinuity distribution, which can be written in a general form as:

$$D_i(\varepsilon) = N_1(\varepsilon)D_i^1 + N_2(\varepsilon)D_i^2 + N_3(\varepsilon)D_i^3, \quad i = x, y \qquad (2)$$

Where, D_i^1, D_i^2, and D_i^3 are the quadratic nodal displacement discontinuities, and,

$$N_1(\varepsilon) = \varepsilon(\varepsilon - 2a_1)/8a_1^2, \quad N_2(\varepsilon) = -(\varepsilon^2 - 4a_1^2)/4a_1^2, \quad N_3(\varepsilon) = \varepsilon(\varepsilon + 2a_1)/8a_1^2 \qquad (3)$$

are the quadratic collocation shape functions using $a_1 = a_2 = a_3$. A quadratic element has 3 nodes, which are at the centers of its three sub-elements.

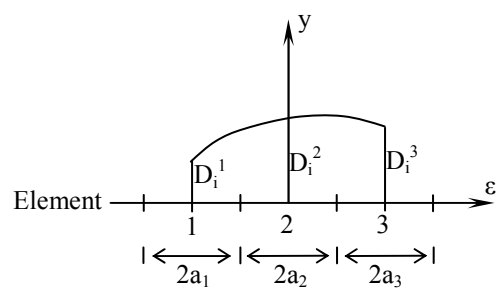

Fig. 2. Quadratic collocations for the higher order displacement discontinuity elements.

The displacements and stresses for a line crack in an infinite body along the x-axis, in terms of single harmonic functions g(x,y) and f(x,y), are given by Crouch and Starfield (1983) as:

$$u_x = \left[2(1-\nu) f_{,y} - y f_{,xx}\right] + \left[-(1-2\nu) g_{,x} - y g_{,xy}\right]$$
$$u_y = \left[(1-2\nu) f_{,x} - y f_{,xy}\right] + \left[2(1-\nu) g_{,y} - y g_{,yy}\right] \quad (4)$$

and the stresses are

$$\sigma_{xx} = 2\mu\left[2 f_{,xy} + y f_{,xyy}\right] + 2\mu\left[g_{,yy} + y g_{,yyy}\right]$$
$$\sigma_{yy} = 2\mu\left[-y f_{,xyy}\right] + 2\mu\left[g_{,yy} - y g_{,yyy}\right] \quad (5)$$
$$\sigma_{xy} = 2\mu\left[2 f_{,yy} + y f_{,yyy}\right] + 2\mu\left[-y g_{,xyy}\right]$$

μ is shear modulus and, $f_{,x}$, $g_{,x}$, $f_{,y}$, $g_{,y}$, etc. are the partial derivatives of the single harmonic functions f(x,y) and g(x,y) with respect to x and y, in which these potential functions for the quadratic element case can be find from:

$$f(x,y) = \frac{-1}{4\pi(1-\nu)} \sum_{j=1}^{3} D_x^j F_j(I_0, I_1, I_2) \ ,$$
$$g(x,y) = \frac{-1}{4\pi(1-\nu)} \sum_{j=1}^{3} D_y^j F_j(I_0, I_1, I_2) \quad (6)$$

in which, the common function F_j, is defined as:

$$F_j(I_0, I_1, I_2) = \int N_j(\varepsilon) \ln\left[(x-\varepsilon) + y^2\right]^{\frac{1}{2}} d\varepsilon, \quad (7)$$
$$j = 1, \text{ to } 3$$

where, the integrals I_0, I_1 and I_2 are expressed as follows:

$$I_0(x,y) = \int_{-a}^{a} \ln\left[(x-\varepsilon)^2 + y^2\right]^{\frac{1}{2}} d\varepsilon = \quad (8\text{-a})$$
$$y(\theta_1 - \theta_2) - (x-a)\ln(r_1) + (x+a)\ln(r_2) - 2a$$

$$I_1(x,y) = \int_{-a}^{a} \varepsilon \ln\left[(x-\varepsilon)^2 + y^2\right]^{\frac{1}{2}} d\varepsilon = \quad (8\text{-b})$$
$$xy(\theta_1 - \theta_2) + 0.5\left(y^2 - x^2 + a^2\right)\ln\frac{r_1}{r_2} - ax$$

$$I_2(x,y) = \int_{-a}^{a} \varepsilon^2 \ln\left[(x-\varepsilon)^2 + y^2\right]^{\frac{1}{2}} d\varepsilon =$$
$$\frac{y}{3}(3x^2 - y^2)(\theta_1 - \theta_2) + \frac{1}{3}(3xy^2 - x^3 + a^3)\ln(r_1) \quad (8\text{-c})$$
$$-\frac{1}{3}(3xy^2 - x^3 - a^3)\ln(r_2) - \frac{2a}{3}(x^2 - y^2 + \frac{a^2}{3})$$

The terms θ_1, θ_2, r_1 and r_2 in this equation are defined as:

$$\theta_1 = \arctan(\frac{y}{x-a}), \quad \theta_2 = \arctan(\frac{y}{x+a}),$$
$$r_1 = \left[(x-a)^2 + y^2\right]^{\frac{1}{2}}, and\ r_2 = \left[(x+a)^2 + y^2\right]^{\frac{1}{2}}$$

STRESS INTENSITY FACTOR AND CRACK TIP ELEMENT

The 'stress intensity factor' is an important concept in fracture mechanics. Considering a body of arbitrary shape with a crack of arbitrary size, subjected to arbitrary tensile and shear loadings (i.e. the mixed mode loading I and II), the stresses and displacements near the crack tip are given in general text books (e.g. Rosmanith 1983, Whittaker et al 1992), but as we use the displacement discontinuity method here we need the formulations given for the SIF (K_I and K_{II}) in terms of the normal and shear displacement discontinuities (Whittaker et al 1992, Scavia 1995).

Based on LEFM theory, the Mode I and Mode II stress intensity factors K_I and K_{II} can be written in terms of the normal and shear displacement discontinuities as (Shou and Crouch 1995):

$$K_I = \frac{\mu}{4(1-\nu)}\left(\frac{2\pi}{a}\right)^{\frac{1}{2}} D_y(a), \quad (9)$$
$$K_{II} = \frac{\mu}{4(1-\nu)}\left(\frac{2\pi}{a}\right)^{\frac{1}{2}} D_x(a)$$

Analytical solution to crack problems for various loading conditions show that the stresses at the distance r from the crack tip always vary as $r^{-1/2}$ if r is small. Due to the singularity variations, $1/\sqrt{r}$ and $\sqrt{r}$ for the stresses and displacements at the vicinity of the crack tip the accuracy of the displacement discontinuity method decreases, and usually a special treatment of the crack at the tip is necessary to increase the accuracy and make the method more efficient. A special crack tip element which already has been introduced in literature (e.g. shou and Crouch 1995) is used here, to represent the singularity feature of the crack tip. Using the special crack tip element of length 2a, as shown in Fig. 3, the parabolic displacement discontinuity variations along this element are given as:

$$D_i(\varepsilon) = D_i(a)(\varepsilon/a)^{\frac{1}{2}}, \quad i = x, y \quad (10)$$

Where, ε is the distance from crack tip and $D_y(a)$ and $D_x(a)$ are the opening (normal) and sliding (shear) displacement discontinuities at the center of special crack tip element.

Substituting equation (10) into equations (4) and (5), the displacements and stresses can be expressed in terms of $D_i(a)$.

The potential functions $f_C(x,y)$ and $g_C(x,y)$ for the crack tip element can be expressed as:

$$f_C(x,y) = \frac{-1}{4\pi(1-\nu)} \int_{=a}^{a} \frac{D_x(a)}{a^{\frac{1}{2}}} \varepsilon^{\frac{1}{2}} \ln\left[(x-\varepsilon)^2 + y^2\right]^{\frac{1}{2}} d\varepsilon$$

$$g_C(x,y) = \frac{-1}{4\pi(1-\nu)} \int_{=a}^{a} \frac{D_y(a)}{a^{\frac{1}{2}}} \varepsilon^{\frac{1}{2}} \ln\left[(x-\varepsilon)^2 + y^2\right]^{\frac{1}{2}} d\varepsilon \tag{11}$$

These functions have a common integral of the following form:

$$I_C = \int_0^{2a} \varepsilon^{\frac{1}{2}} \ln\left[(x-\varepsilon)^2 + y^2\right]^{\frac{1}{2}} d\varepsilon \tag{12}$$

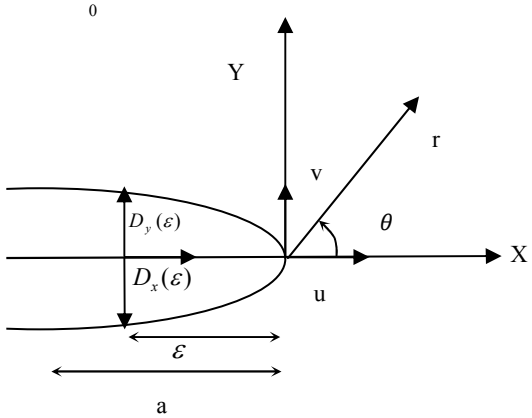

Fig. 3. Displacement correlation technique for the special crack tip element

FRACTURE PROPAGATION CRITERION

The mixed mode of stress intensity factors (i.e. Mode I and Mode II fractures, which are the most commonly fracture modes occur in rock fracture mechanics) are numerically computed. Several mixed mode fracture criteria has been used in literature to investigate the crack initiation direction and its path (Shen and Stephansson 1994; Whittaker et al., 1992; Rao et al., 2003). As most of rocks are brittle and weak under tension the Mode I fracture toughness KIC (under plain strain condition) with the maximum tangential stress fracture criterion (σ-criterion) introduced by Erdogan and Sih are used to predict the crack propagation direction (Erdogan and Sih, 1963). This is a widely used mixed mode facture mechanics criterion and well fitted with the experimental results (Ingraffea 1983; Guo et al., 1990; Scavia 1992; Whittaker et al., 1992).

Based on this criterion the crack tip will start to propagate when:

$$\cos\frac{\theta_0}{2}\left[K_I \cos^2\frac{\theta_0}{2} - \frac{3}{2}K_{II}\sin\frac{\theta_0}{2}\right] = K_{IC} \tag{13}$$

Where θ_0 is the crack propagation angle follows that

$$\theta_0 = 2\arctan\left[\frac{1}{4}\left(\frac{K_I}{K_{II}}\right) - \frac{1}{4}\sqrt{\left(\frac{K_I}{K_{II}}\right)^2 + 8}\right] \tag{14}$$

The latter value corresponding to the crack tip should satisfy the condition:

$$K_I \sin\theta_0 + K_{II}(3\cos\theta_0 - 1) = 0 \tag{15}$$

A fracture propagation model completes when, the fracture increment length of a crack can be predicted. This can be done by two ways: (i) predicting fracture increment length for a given loading condition and (ii) predicting the load change required to extend a crack for a given length (Ingraffea., 1987).

For a given crack length of 2b, under a certain loading condition, the crack propagation angle θ_0 is predicted (based on LEFM principles and σ-Criterion i.e. equations (13) and (14)). Then the original crack is extended by an amount Δb that has equal length with crack tip element. This element will be perpendicular to the maximum tangential stress near the crack tip. So a new crack length $2(b+\Delta b)$ is obtained and again the equations (13) and (14) are used to predict the new conditions of crack propagation for this new crack. This procedure is repeated until the crack stops its propagation or the material breaks away. This procedure can give a propagation path for a given crack under a certain loading condition.

VERIFICATION OF HIGHER ORDER DISPLACEMENT DISCONTINUITY

Verification of this method is made through the solution of several example problems i.e. a pressurized crack in an infinite body, inclined crack in a infinite body, a circular arc crack under biaxial tension in infinite bodies and oriented pressurized crack under compressive far field stresses. Therefore, the accuracy of the method is demonstrated by example problems because the results are in good agreement with the analytical solutions.

A pressurized crack in an infinite plane

Because of its simple solution, the problem of a pressurized crack has been used for the verification of the numerical methods developed here. The analytical solution of this problem has been derived and explained by Sneddon (1951). Based on Figure 4, the analytical solution for the normal displacement

discontinuity D_y along the crack boundary, and the normal stress σ_y near the crack tip ($|x| > b$), can be written as

$$D_y = -\frac{2(1-\upsilon)P}{\mu}(b^2 - x^2), |x| > b$$
$$\sigma_y = -\frac{P_x}{(x^2 - b^2)^{0.5}} - P, |x| > b \qquad (16)$$

where ϑ is the Poisson's ratio of the body. Consider a pressurized crack of a half length b = 1 m, under a normal pressure P=-10 MPa, with a modulus of elasticity E=2.2 GPa, and a Poisson's ratio ϑ=0.1(Fig. 4). The normalized displacement discontinuity distribution $\frac{D_y}{b} \times 10^3$ along the surface of the pressurized crack are given in Figure.5 using the constant (ordinary) displacement discontinuity program TWODD (Crouch and Starfield, 1983) and higher order displacement discontinuity program TDDQCR. As shown in this figure by using special crack tip element, the percent error of displacement discontinuity D_y will be reduced. Therefore using this higher order program for calculating the normalized displacement discontinuity distribution $D_y/b \times 10^3$ along the surface of the pressurized crack, gives results that are more accurate.

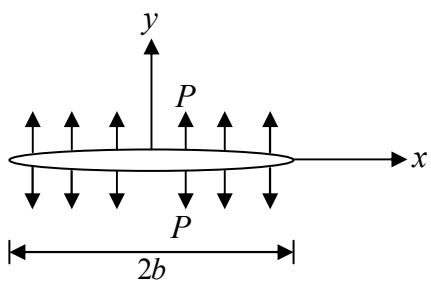

Fig.4. A pressurized crack in an infinite plane

The normalized normal stress (σ_{yy}/P) near the crack tip and along the x-axis of the pressurized crack is presented in figure.6. The overall results show that the program using quadratic elements (i.e. TDDQCR) gives more accurate results compared to the program using constant elements (i.e. TWODD).

Normal stress (σ_{yy}) field distribution around of the pressurized crack is shown in Figure.7. The stresses near the crack tips are tensional that have positive sign and stresses around the wall of crack are compressive that have negative sign. Like Figure.6, the normal stresses near the crack tips are calculated about five times more than pressure inside the crack.

Curved cracks under biaxial tension in infinite plane

Curved and kink cracks may occur in cracked bodies (Shou and Crouch, 1995). The proposed method is applied to the problem of different degrees of circular arc crack under far field biaxial tension (Figure. 8). Analytical values of the Mode I and Mode II stress intensity factors, KI and KII, and strain release rate, G for a general circular arc crack under biaxial tension given by Cotterell and Rice (1980) as

$$K_I = \sigma \cos\frac{\alpha}{4}\left[\frac{\pi r \sin\frac{\alpha}{2}}{1+\sin^2\frac{\alpha}{4}}\right]^{0.5}$$
$$K_{II} = \sigma \sin\frac{\alpha}{4}\left[\frac{\pi r \sin\frac{\alpha}{2}}{1+\sin^2\frac{\alpha}{4}}\right]^{0.5} \qquad (17)$$
$$G = \frac{1-\vartheta^2}{E}(K_I^2 + K_{II}^2)$$

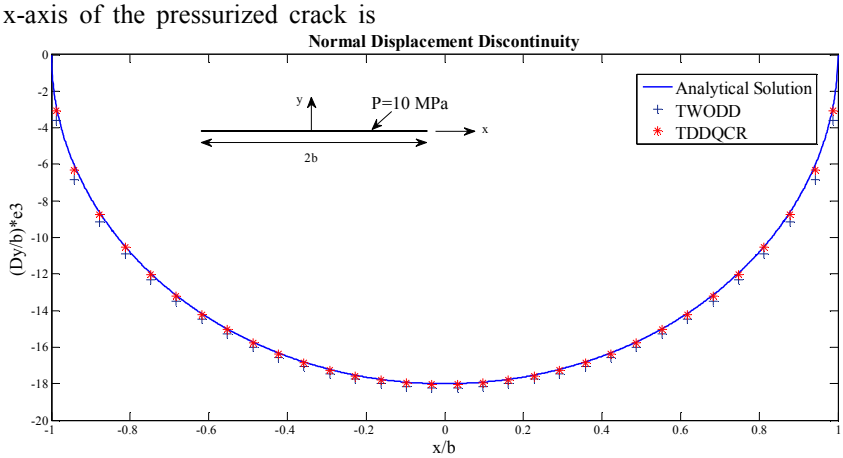

Fig.5. Normal displacement discontinuity distribution along the pressurized crack in an infinite plane

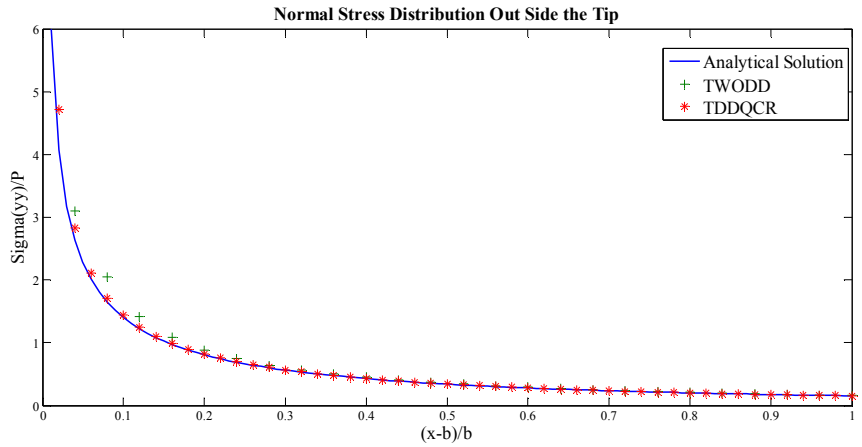

Fig.6. Normal stress distribution outside the tip of the line pressurized crack (along y=0).

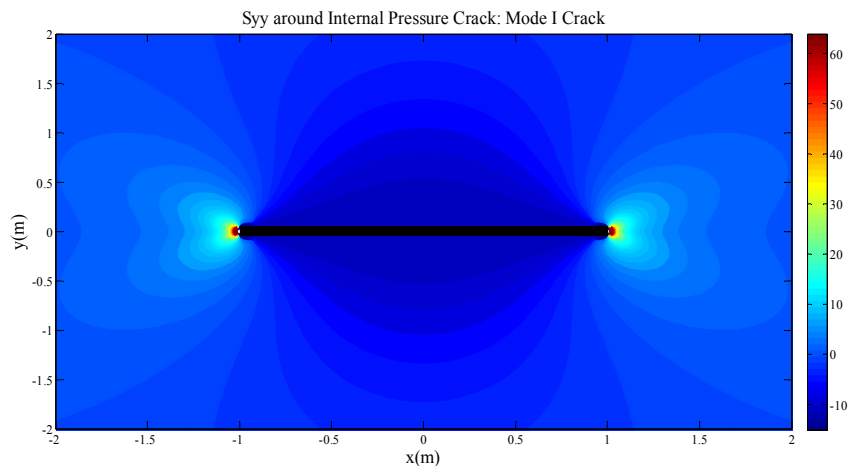

Fig.7. Normal stress (σ_{yy}) distribution around of the pressurized crack.

Different degrees of circular arc crack under biaxial tension, σ=10 MPa with a radius of r=1 m are considered. The modulus of elasticity and Poisson's ratio of the material are taken as E=10 GPa and ϑ=0.2. The numerical solution of this problem has been obtained by using a higher order displacement discontinuity programs TDDQCR (using one special crack tip element at each crack end) and using 50 nodes along the crack.

A circular arc crack under biaxial tension has been solved to show the validity of the results obtained by using the higher order displacement discontinuity program TDDQCR. The numerical values for strain energy release rate (G) are given in Figure.9. Comparing the numerical and analytical values (i.e. the values of strain energy release rate, G) calculated for this problem proves the validity and accuracy of the numerical results for curved crack problems too.

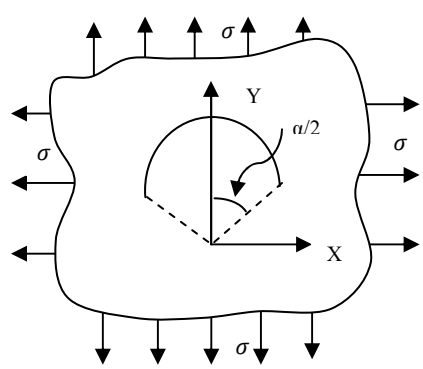

Fig.8. Circular arc crack under uniform biaxial tension.

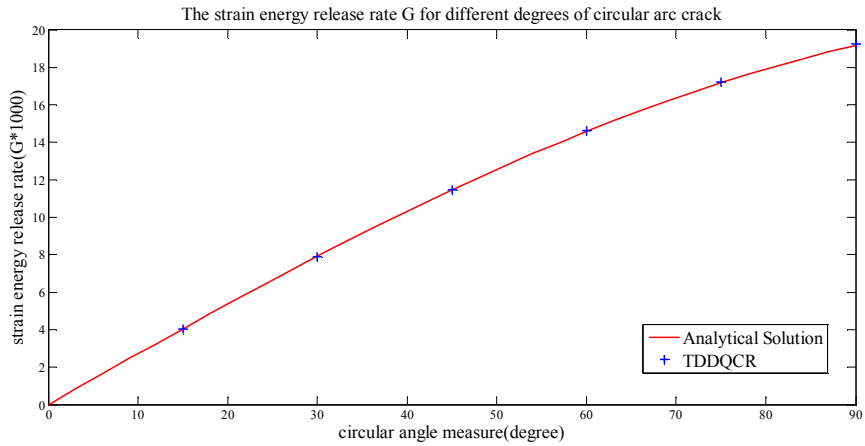

Fig.9. The strain energy release rate, G for different degrees of circular arc crack

Slanted crack in an infinite body

Another verification of this method is made through the solution of a center-slanted crack in an infinite body that is shown in Figure.10. The slant angle,β, changes counterclockwise from the x (horizontal) axis, and the tensile stress σ=10 MPa is acting parallel to the x axis. A half crack length b=1 meter, modulus of elasticity E=10 GPa, Poisson's ratio ν=0.2, fracture toughness K_{IC}=2 MPa√m are assumed. The analytical solution of the first and second mode stress intensity factors K_I and K_{II} for the infinite body problem are given as (Guo et al 1990, Whittaker et al 1992):

$$K_I = \sigma(\pi b)^{\frac{1}{2}} \sin^2\beta \;\Rightarrow \frac{K_I}{\sigma\sqrt{\pi b}} = \sin^2\beta$$
$$K_{II} = \sigma(\pi b)^{\frac{1}{2}} \sin\beta\cos\beta \Rightarrow \frac{K_{II}}{\sigma\sqrt{\pi b}} = \sin\beta\cos\beta \qquad (18)$$

The numerical and analytical results obtained for this problem show the accuracy and usefulness of the higher order quadratic displacement discontinuity program TDDQCR designated for the treatment of the crack problems. A total number of 152 nodes, and a crack tip length to half crack length ratio, L/b=0.1 have been used for the numerical solution of the problem.

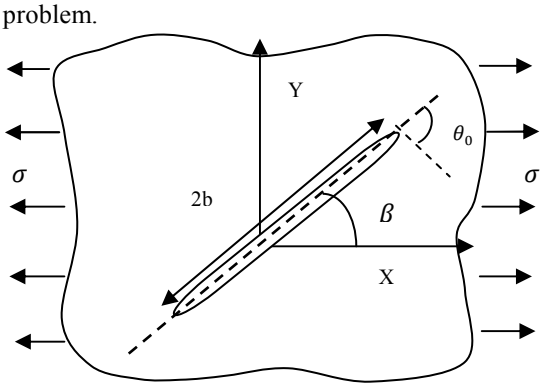

Fig.10. Center slanted cracks in an infinite body under far field tension

Equation (13) and (14) reveal that θ_0 is a function of the ratio K_I / K_{II} and the crack inclination angle β, since KI and KII are functions of β (equation 18 and Figures 11 and 12). Because of its simplicity, the center slant crack problem has been solved by different investigators e.g. Guo, et. al (1990) used the constant element displacement discontinuity with a special crack tip element for angles 30, 40, 50, 60, 70 and 80 degrees. They used a different fracture criterion, for evaluating the crack initiation angle θ_0 and compared their results with the results obtained by other researchers using different fracture theories. Figure 13 compares the variation of θ_0 that obtained from higher order displacement discontinuity programs using the maximum tangential stress theory proposed by Erdogan and Sih (1963), and the results obtained by σ-criterion. The numerical results obtained here are very close to those predicted by the σ-criterion.

Oriented pressurized crack under far field stress

For verification of numerical method in compressive biaxial loading, the pressurized crack that is oriented at an arbitrarily angle β with respect to the direction of the maximum principal stress, σ_H is studied (Figure 14). For such loaded crack, both the mode I and II stress intensity factors exist at the crack tips, which have been given by (Rice, 1968) as follows:

$$K_I = \sqrt{\pi a}\left[P - (\sigma_H \sin^2\beta + \sigma_h \cos^2\beta)\right]$$
$$K_{II} = \frac{\sqrt{\pi a}}{2}\left[\sigma_H - \sigma_h\right]\sin 2\beta) \qquad (19)$$

Where a is the half crack length and P is the internal pressure.

The conditions and geometry for numerical solution are the maximum horizontal stress = -7 MPa, the minimum horizontal stress = -2 MP, pressure inside the fracture P=-10 MPa, and the half of crack length b=1m. Properties of material are modulus of

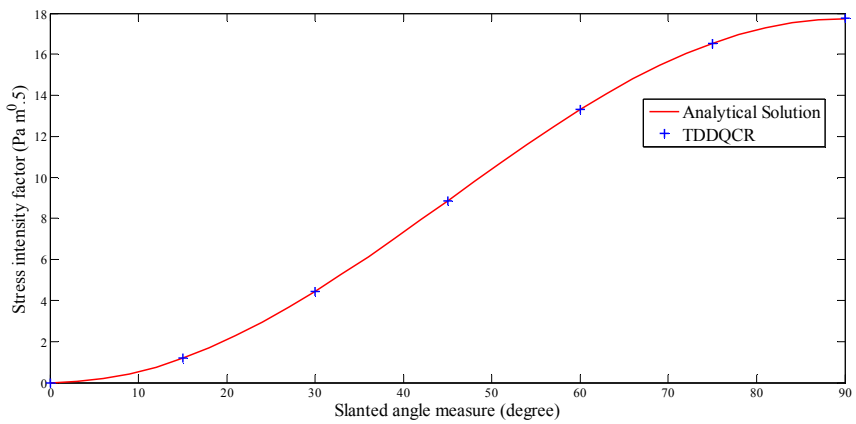

Fig.11. Analytical and numerical values of the stress intensity factors, K_I for the inclined crack at different orientation from the horizontal axis (X-axis), for L/b= 0.1 and 152 nodes.

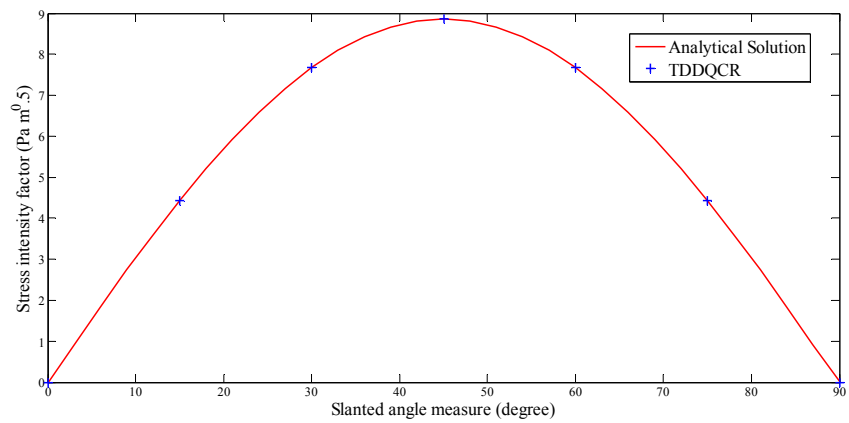

Fig.12. Analytical and numerical values of the stress intensity factors, K_{II} for the inclined crack at different orientation from the horizontal axis (X-axis), for L/b= 0.1 and 152 nodes.

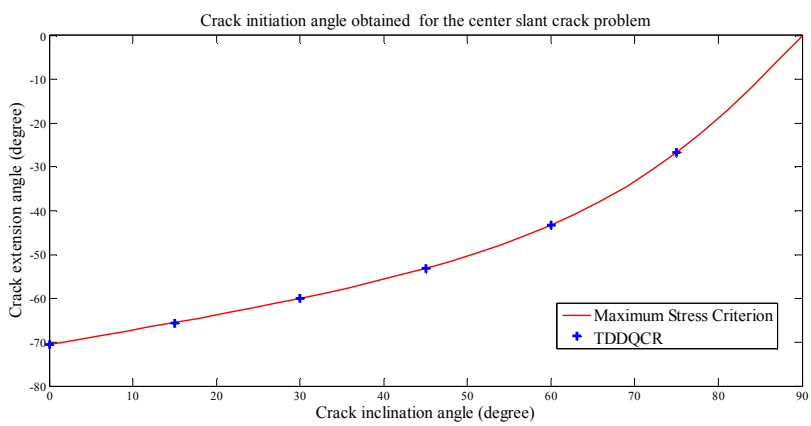

Figure. 13. Crack propagation angle θ_0 as a function of crack inclination angle β

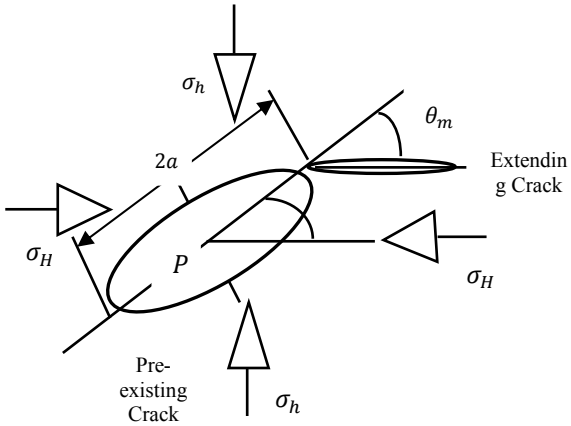

Fig. 14. Arbitrarily oriented crack under far field stresses and internal pressure

elasticity E = 10 GPa, Poisson's ratio t = 0.2, and Mode I fracture toughness KIC = 2 MPa $m^{1/2}$. The ratio of crack tip element length l to the crack length b is 0.05. Figure 15 shows the good agreement between the numerical results and analytical results from the literature for both of stress intensity factors KI and KII.

CRACK INTERACTION

A better understanding of how an induced fracture interacts with a discontinuity is fundamental for predicting the ultimate size and shape of the hydraulic fractures formed by a treatment. It can be found that the stresses between two tips of cracks have an influence on the crack propagation and consequently deviate it and the path of fracture will be changed with alteration in distance and inclination. For that reason, hydraulic fracturing propagation path for different inclination angles of discontinuity in two distances is studied (Figure.16). The physical properties are E=10 GPa, $\vartheta = 0.25$, K=2 MPa.$m^{0.5}$. The maximum compressive horizontal stress (X-axis) and minimum compressive horizontal stress (Y-axis) are 7 and 2 MPa respectively, and the pressure inside the fracture is 10 MPa. Figure 17 shows the paths of hydraulic fracturing for distance 2c=2a. The path of fracture when interacts with discontinuity with 90-degree inclination is in straight line, but with decreasing in the inclination angle, the fracture deviates from its direction and reorients sooner. Discontinuity changes the field stress near its surface and causes the principal stresses to be locally parallel and perpendicular to the surface, therefore all fractures tend to interact with discontinuity at right angle.

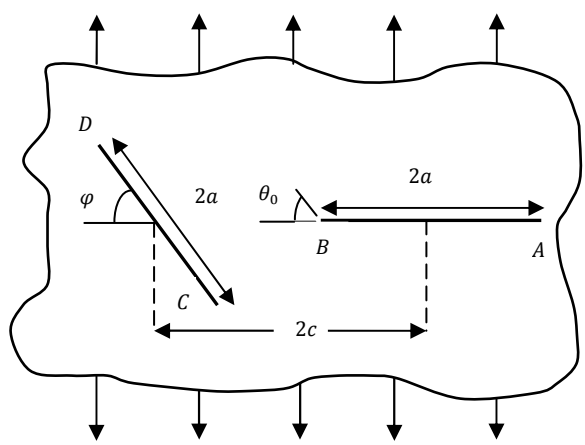

Fig. 16. Two equal inclined cracks

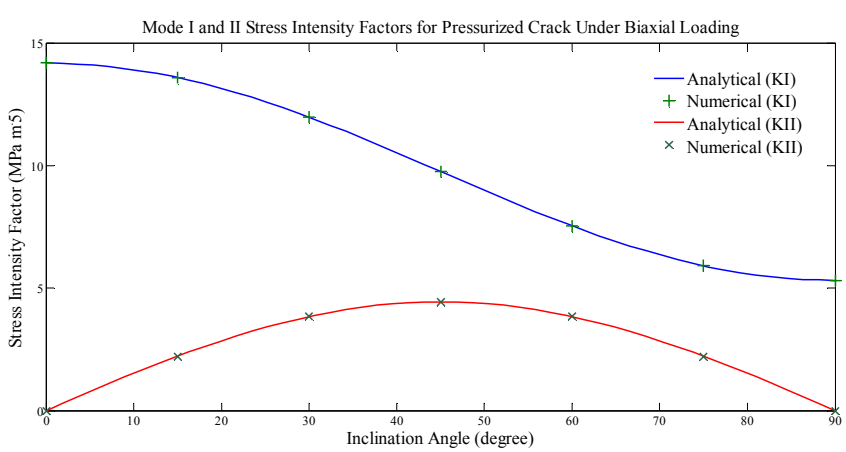

Fig. 15. Analytical and numerical values of the stress intensity factors,K_I and K_{II} for the inclined pressurized crack at different orientation from the maximum horizontal stress (X-axis).

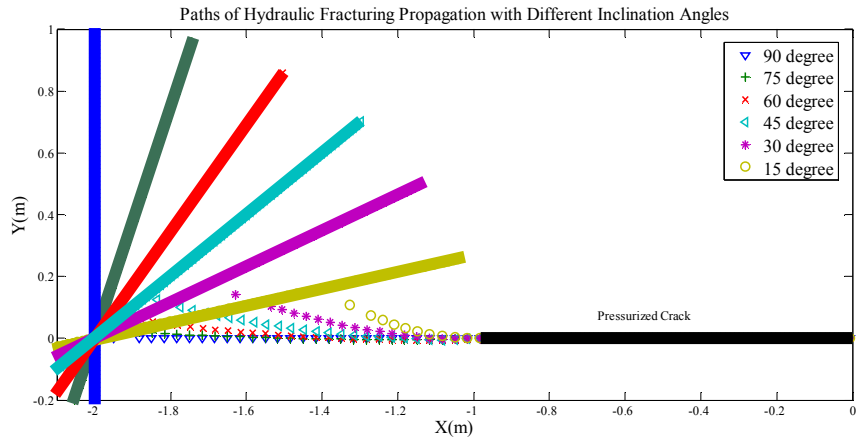

Fig. 17. Hydraulic fracturing propagation paths for different inclination angles of inclined discontinuity with distance c/a=1.

Discontinuities that are parallel with pressurized fracture influence the propagation of fracture. In this study the effect of spacing between the parallel discontinuity and pressurized crack in X and Y direction is considered. The properties of material and stress condition are same that mentioned before. The geometry and results are shown in Figure 18 and 19. For the first example (Figure 18), the distance between the discontinuity and fracture is changed in X direction and the distances in Y direction are constant. The results show when the fracture propagates under discontinuity, the path of fracture deviates towards the discontinuity and then propagates in its direction, but finally level of propagation will change and has a jump.

In the second example (Figure 19), the distance between the discontinuity and fracture is changed in Y direction and the distances in X direction will be constant. Results show with increasing the distance in Y direction the influence of discontinuity on propagation path will be less and fracture tend to propagate near its plane, therefore for different distances fracture propagates in different level.

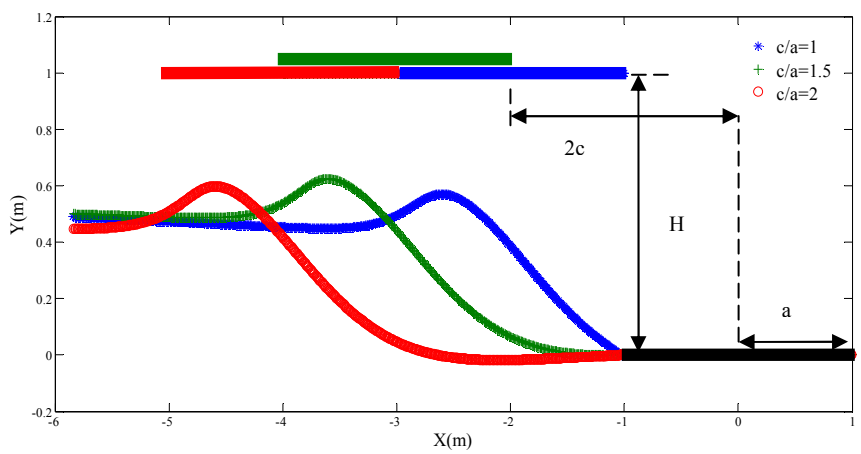

Fig. 18. Paths of pressurized crack that is parallel to discontinuity for different distances in X Direction. P=-10 MPa, σ_H=-7 MPa, σ_h =-2 MPa, and H/a=1

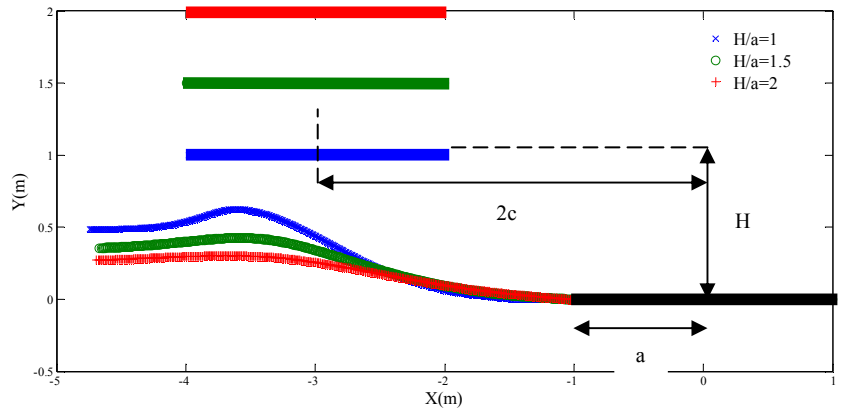

Fig. 19. Paths of pressurized crack that is parallel to discontinuity for different distances in Y Direction. P=-10 MPa, σ_H=-7 MPa, σ_h =-2 MPa, and c/a=1.5.

CONCLUSION

A numerical method is presented in this paper for mixed-mode crack tip propagation of pressurized fractures in remotely compressed rocks. The maximum tangential stress criterion is implemented sequentially to trace the crack propagation path. Results from this numerical method are compared with that available in the literature showing that the results have good agreement with the analytical solutions.

Stress intensity factors computed by the approximate method are very close to that obtained from analytical solution for the fracture-stress system studied in this paper. Crack tip propagation angles obtained from the proposed numerical method are compared with that available in the literature, and good agreements are obtained.

It is found that the position, distance, and inclination of the hydraulic fracture relative to the pre-existing discontinuity have a strong influence on the fracture propagation path.

REFERENCES

Albright, J., and Pearson, C., 1982. Acoustic emissions as a tool for hydraulic fracture location: Experience at the Fenton hill hot dry rock site, SPE ATCE, Dallas, Sept. 21-24, Paper 9509.

Aliabadi, M.H., 1998. Fracture of Rocks. Computational Mechanics Publications, Southampton, UK.

Aliabadi, M.H., Rooke, D.P., 1991. Numerical Fracture Mechanics. Computational Mechanics Publications, Southampton, UK.

Ching, H.Y., 1997. Mechanics of Hydraulic Fracturing. Gulf Publishing Company, Texas.

Clark, J. B., 1949. "A hydraulic process for increasing the productivity of wells", Petroleum Trans. American Institute of Mining and Energy, v. 186, p. 1-8.

Cotterell, B., Rice, J.R., 1980. Slightly curved or kinked cracks. Int. J. Fract. Mech. 16, 155–169.

Crawford, A.M., Curran, J.H., 1982. Higher order functional variation displacement discontinuity elements. Int. J. Rock Mech. Miner.Sci. Geomech. Abstr. 19, 143–148.

Crouch, S.L., 1976. Solution of plane elasticity problems by the displacement discontinuity method. Int. J. Numer. Methods Eng. 10, 301–343.

Crouch, S.L., Starfield, A.M., 1983. Boundary Element Methods in Solid Mechanics. Allen and Unwin, London.

Erdogan, F., Sih, G.C., 1963. On the crack extention in plates under plane loading and transverse shear, J. Basic Engin. 85, 519-527

Guo, H., Aziz, N.I., Schmidt, R.A., 1990. Linear elastic crack tip modeling by displacement discontinuity method. Eng. Fract. Mech. 36, 933–943.

Hossaini Nasab H., Marji M. F., 2007., A Semi-Infinite Higher-Order Displacement Discontinuity Method and its Application to the Quasistatic Analysis of Radial Cracks Produced by Blasting., J. Mechanics of Materials and Structures, Vol. 2, No. 3.

Ingraffea A. R., 1983. Numerical Modeling of Fracture Propagation, In: Rock Fracture Mechanics, Rossmanith H. P. (Editor); Springer Verlagwien; New York, pp. 151-208.

Ingraffea, A.R., 1987. Theory of crack initiation and propagation in rock. In: Atkinston, B.K. (Ed.),

Fracture Mechanics of Rock, Geology Series. Academy Press, New York, pp. 71–110, pp. 151–208.

Marji M. F., Dehghani I., 2009., Kinked Crack Analysis by A Hybridized Boundary Element/Boundary Collocation Method., Int. J. of Solids and Structures

Marji M. F., Hosseini_Nasab, H. and Kohsary A. H., 2006. On the uses of special crack tip elements in numerical rock fracture mechanics Int. J. Solids and Struct., 43,1669- 1692.

Rao, Q., Sun, Z., Stephansson, O., Li, C., Stillborg, B., 2003. Shear fracture (Mode II) of brittle rock. Int. J. Rock Mech. Miner. Sci. 40, 355–375.

Rice, J. R. 1968. Mathematical analysis in the mechanics of fracture, Fracture: An Advanced Treatise, Vol. II, H. Liebowitz, Academic Press, New York, NY, pp 191-311.

Rossmanith, H P., 1983., Rock Fracture Mechanics., Springer Verlagwien, New York.

Scavia, C., 1992. A numerical technique for the analysis of cracks subjected to normal compressive stresses. Int. J. Numer. Methods Eng. 33, 929–942.

Scavia, C., 1995. A method for the study of crack propagation in rock structures. Géotechnique 45(3), 447–463.

Shen, B. and Stephansson, O. 1994. Modification of the G-criterion for crack propagation subjected to compression. Engineering Fracture Mechanics 47(2), 177–189.

Shou, K.J., Crouch, S.L., 1995. A higher order displacement discontinuity method for analysis of crack problems. Int. J. Rock Mech. Miner. Sci. Geomech. Abstr. 32, 49–55.

Sneddon, I.N., 1951. Fourier Transforms. McGraw-Hill, New York.

Tan, X.C., Kou, S.Q., Lindqvist, P.A., 1996. Simulation of rock fragmentation by indenters using DDM and fracture mechanics. In: Aubertin, M., Hassani, F., Mitri, H. (Eds.), Rock Mechanics, Tools and Techniques. Balkema, Roterdam.

Whittaker, B.N., Singh, R.N., Sun, G., 1992. Rock Fracture Mechanics, Principles, Design and Applications. Elsevier, The Netherlands.